
Article:
Buckley-Johnstone, L.E., Trummer, G., Voltr, P. et al. (2 more authors) (2020) Full-scale testing of low adhesion effects with small amounts of water in the wheel/rail interface. Tribology International, 141. ISSN 0301-679X

https://doi.org/10.1016/j.triboint.2019.105907

Full-scale testing of low adhesion effects with small amounts of water in the wheel/rail interface

L.E. Buckley-Johnstone[1], G. Trummer[2], P. Voltr[3], K. Six[2], R. Lewis[1],

[1]Department of Mechanical Engineering, The University of Sheffield, Sheffield, UK
[2]Virtual Vehicle Research Center, Graz, Austria
[3]Jan Perner Transport Faculty, University of Pardubice, Pardubice, Czech Republic

Abstract

Low adhesion in the wheel/rail contact can be caused by small amounts of water combining with iron oxides. This happens in light rain or at dew point. In small-scale tests, ultra-low adhesion (≤0.05) has not been maintained. The aim here was to see if the mechanism could be realized at a larger scale. Sustained ultra-low adhesion was achieved when water was applied constantly to the wheel/rail contact at a rate of 25µL/s. In these conditions wear debris and oxide was clearly visible in the contact band. Creep force data has been generated that can now be used to inform wheel/rail contact models and multi-body dynamics simulations of train behaviour with a view to developing mitigation.

1 Introduction

Low adhesion is a serious problem for railway networks. In braking it causes safety problems as it can lead to Signals Passed at Danger (SPADs) and station overruns as brakes fail to stop trains. In the worst case these can lead to collisions. In traction it poses a different problem, as failure to accelerate as required can cause delays to a train. Both these can be very costly.

Work carried out to analyse the frequency of the braking related incidents during the autumn period has shown that the cause is split 50:50 between leaves and 'wet-rail' syndrome [1]. Wet-rail syndrome relates to low adhesion caused by the presence of small amounts of water along with some solid material, such as oxides generated naturally in the wheel/rail interface.

Far more work has been carried out to study the effects of leaves than wet-rail. A recent review encapsulates much of this [2]. Investigations have been carried out to characterise the role of water on friction (for example see [3]). Ultra-low friction (<0.05) is only achieved when surfaces are very smooth in conditions rarely seen in the wheel/rail interface. Studies involving oxides have largely focussed on wear (see [4]), but where they have looked at friction ultra-low levels have not been measured [4-8].

Looking at the timing of the incidents revealed that most wet-rail occurred during the morning and evening dew point, where a thin film of water would have been present on the rail head. Measurements on a rail head in an environment chamber have revealed that this amount was approximately 0.01 – 0.68 µL per 100 mm^2 [9].

Twin disc experimental testing showed that friction decreased in a drying contact where there was a small amount of water mixed with oxides [10] (see Figure 1). Similar testing using a different type of test (High Pressure Torsion (HPT)) has

shown similar effects [9] (see Figure 2). Here friction clearly dropped as the amount of water applied was reduced. Neither, however, showed a drop to ultra-low adhesion conditions that would lead to braking problems (<0.05). Physical modelling of the HPT testing (see Figure 3) showed that it would be very difficult to achieve the exact conditions required for very low adhesion as only a small range of water/oxide mixture proportions leads to this occurring [9].

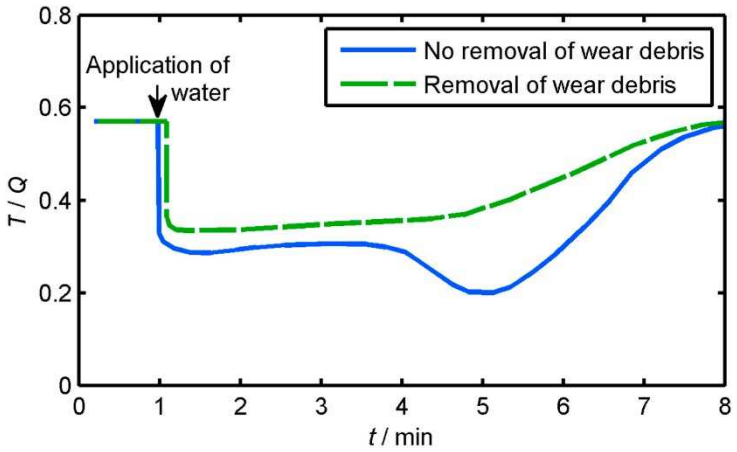

Figure 1: Results from Amsler twin disc experiments showing that Wear Debris (iron oxides) are necessary to Significantly Reduce the Adhesion Level (data from Beagley & Pritchard [10] figure from Trummer et al. [11])

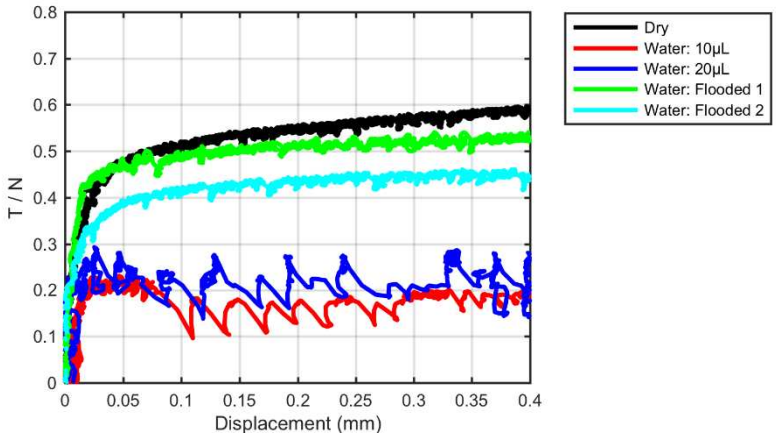

Figure 2: Effect of a range of amounts of water on a HPT test. Dry data has been plotted for comparison. Normal pressure: 600 MPa [9]

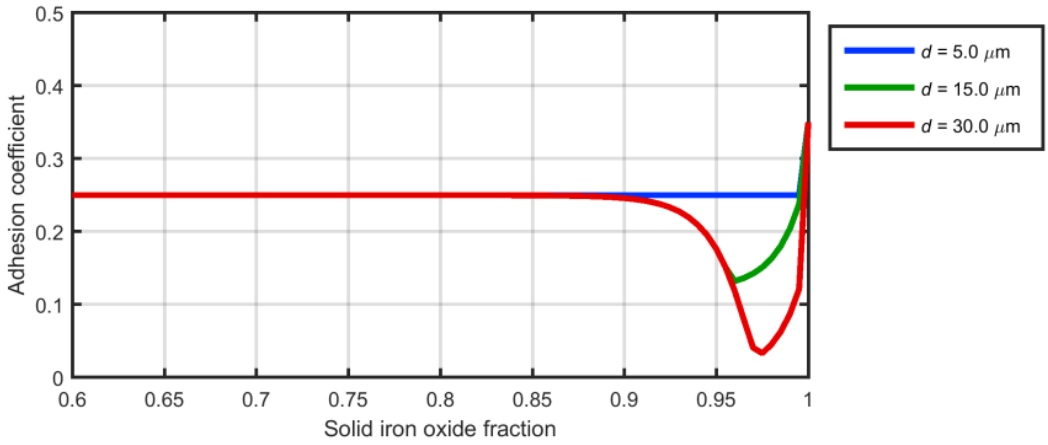

Figure 3: Physical modelling of adhesion against water/oxide mixture proportion in HPT test interface for different amounts/heights (d) of water/oxide mixture [9]

It was thought that it might be easier to study the mechanisms using a full-scale test approach. The larger contact would make it easier to achieve the small amounts of water required over that possible in the scaled approaches mentioned above. No full-scale work in the literature has achieved ultra-low adhesion using water and oxide mixtures. The aim of this work was to create ultra-low adhesion conditions in a full-scale rig and determine creep force characteristics for a range of different water amounts.

2 Experimental Details

2.1 Test Apparatus

Tests have been carried out at the Jan Perner Transport Research Centre at the University of Pardubice. The test rig comprises a full-scale tram wheel (Ø700 mm) mounted onto a fixed frame by a swing arm and a roller 'rotating rail' (Ø916 mm) mounted below. An air spring between the swing arm and main frame is used to apply a normal load between the wheel and rail. The wheel is driven by a permanent magnet synchronous motor with torque control, whilst the roller is driven by an asynchronous motor to maintain constant speed. A torque sensor located on the rail roller axis is used to measure the torque as a result of the wheel-roller contact throughout testing. Further detail on the test rig can be found in previously published literature [12].

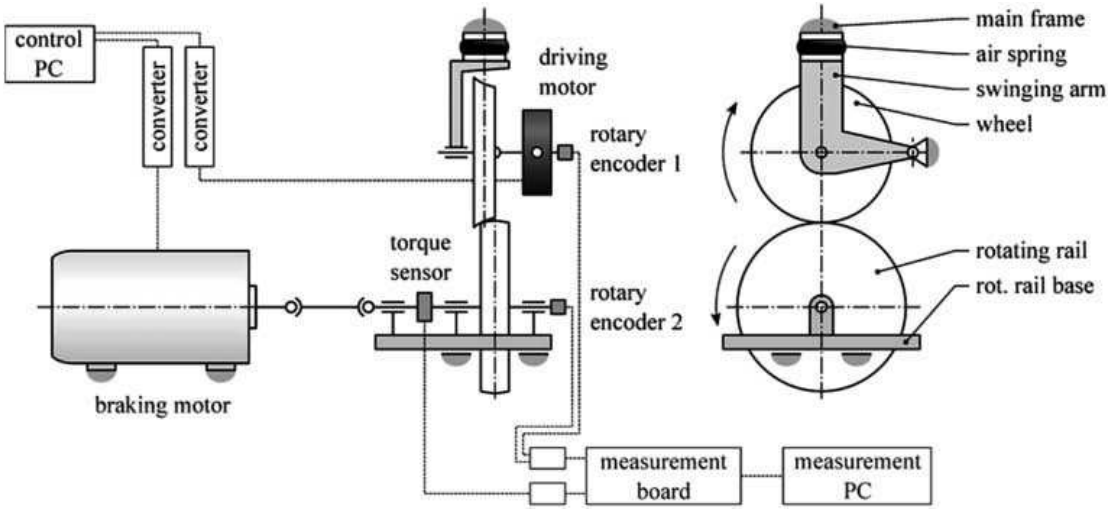

Figure 4: Schematic of the tram wheel test rig [12]

The torque motor is capable of applying up to 850 Nm of torque in braking or traction (equivalent to a 2.4 kN friction force). This limit has a consequence on the creepage range that can be investigated at higher loads. This is due to the longitudinal friction force induced by the maximum motor torque that cannot exceed the creep force at the contact required to get into full sliding under certain conditions. These limits are shown in Table 1.

Table 1: Maximum permissible friction coefficients for different normal loads in the tram wheel/rail rig to achieve full sliding.

Normal load (kN)	Investigation friction (T/N) limit
4	0.60
10	0.24
20	0.12
40	0.06

A typical test history plot is shown in Figure 5. This shows how a test progresses over time: A normal load (N) is applied to the two discs using the air spring. The discs are then accelerated to the test speed of interest. The longitudinal force (T) in the contact is measured by a torque sensor.

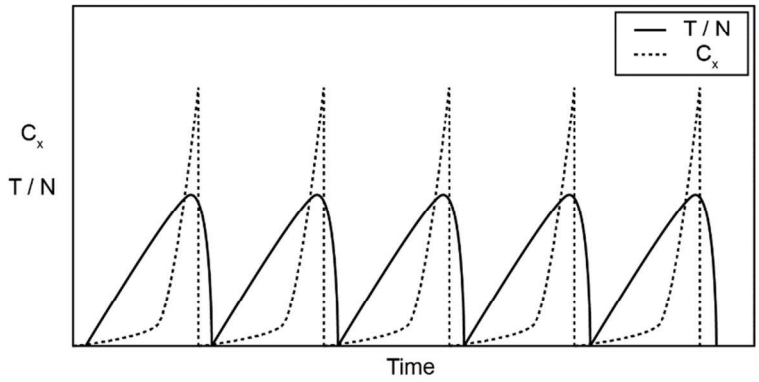

Figure 5: Creepage and coefficient of adhesion data from the tram wheel rig. Plot shows 5 instances of testing where torque is increased until slip occurs

Creep is generated by applying a controlled torque on the wheel roller, while the rail rotates at a fixed speed, until the adhesion limit is exceeded and slippage between wheel and roller occurs.

Instantaneous velocities of the wheel and roller are measured using rotary encoders on each shaft. This allows calculation of longitudinal creep c_x over the duration of a test run, with corresponding measured torque.

$$c_x = \left|\frac{v_{rail} - v_{wheel}}{v_{rail}}\right| \quad (1)$$

If slippage occurs, the prescribed torque is returned to zero and rolling resumes. Multiple creep curves are then generated by increasing the applied torque from zero again until slippage occurs. This can be repeated several times in a single test run (see Figure 5).

Two different application methods to supply water to the contact were used. The first employed a voltage micropump (M100S-180 TCS Micropumps) with options to divert water back into the reservoir for reducing flow rates. This test set up included a nozzle to supply compressed air to clean the contact band post contact. The minimum delivery rate in this set-up was 350 µL/s over an area larger than the contact width. The test schematic is shown in Figure 6.

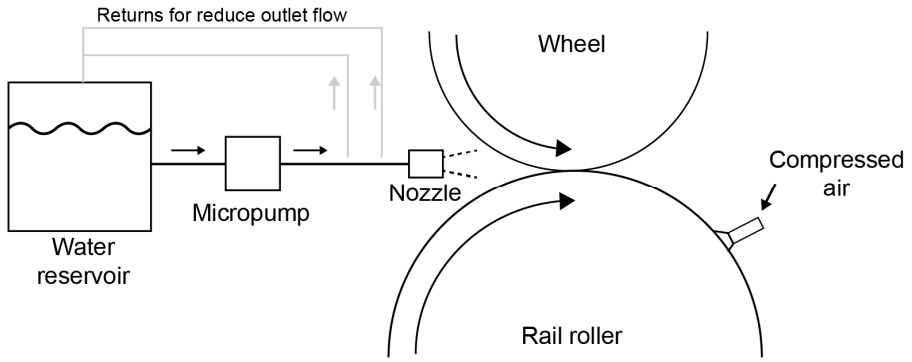

Figure 6: Constant water application test set-up schematic

Constant water and bulk water application tests were performed using the micropump water application system. The compressed air was only used during the constant water application tests.

Application amounts when using the micropump application exceeded ‘low’ amounts. Therefore, tests with constant water applied using controlled application of water drops were performed. The system was a gravity fed water supply through pipe with the outlet directed at the contact band. The average droplet amount was measured at 60 µL/drop. Water drop rate was controlled by adjusting a valve, as shown in Figure 7. No additional contaminants were applied during the water droplet test.

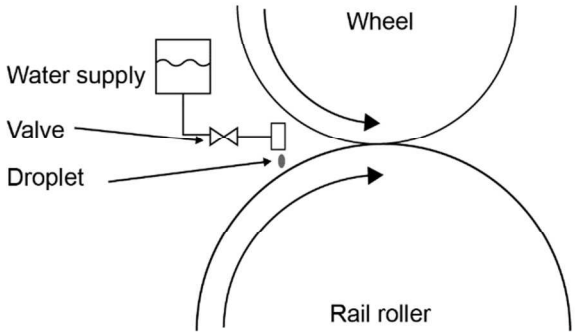

Figure 7: Schematic diagram of the water droplet application system. Droplets applied to rail roller as close as possible to contact

2.2 Methodology

A standard test produces 5 creep curves. However, the test procedure varied depending on the exact conditions under investigation. This variation in procedure arises as testing with contaminants necessitates possible variations in test length and number of cycles. For example, allowing enough time to complete the drying out of water whilst completing creep curves at regular intervals.

In dry conditions it was sufficient to generate 5 creep curves sequentially. The standard procedure for all dry tests was as follows:

1. Apply normal load
2. Accelerate to steady rolling velocity
3. Increase torque until wheel slide initiates, or motor torque limited is reached
4. Torque returned to zero and free rolling resumes
5. Repeat steps 3 and 4 until sufficient amount of creep curves are generated.

When contaminants are investigated, there are additional steps that have been described below.

The set of ‘water + drying with compressed air’ tests used the micropump applicator in conjunction with the compressed air feed. Water was supplied to the running band before entering the contact, and then any water that remained on the running band area was removed by the compressed air. The application of water was started and stopped before and after each cycle (see Figure 8).

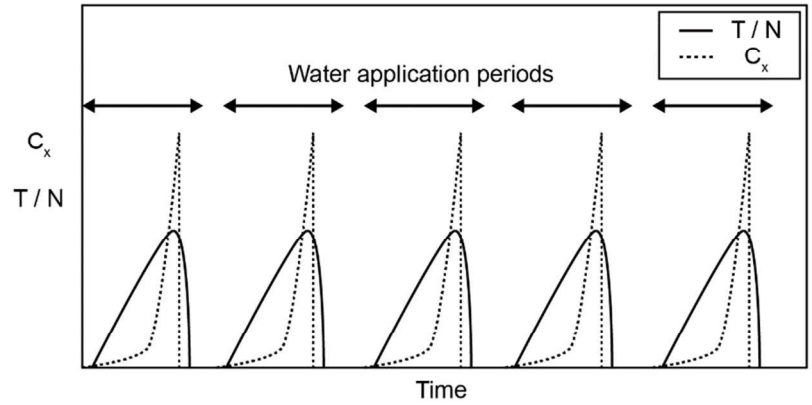

Figure 8: Schematic test timeline for constant water application using micropump + compressed air set-up

The set of bulk water tests used the micropump applicator alone. Cycles were run to check the level of adhesion before any water was applied to the surface. Water was then applied to the roller at 6 ml/s over a period of 10 seconds under free rolling conditions. Steps 3 – 5 were then repeated until the contact band was observed to be dry and the adhesion level had returned to dry values. Figure 9 shows a schematic test time line for bulk water tests.

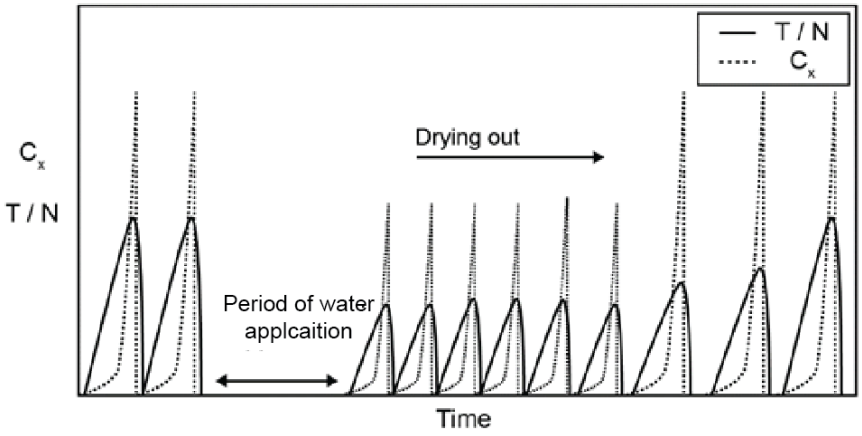

Figure 9: Schematic test timeline for bulk water application tests

The tests for water droplets included two initial curves generated under clean conditions prior to water application followed by constant water application during torque increase and decrease, as shown in Figure 10. In these test conditions water was applied to the contact for 15 cycles then stopped and cycles were then run until dry values were returned to.

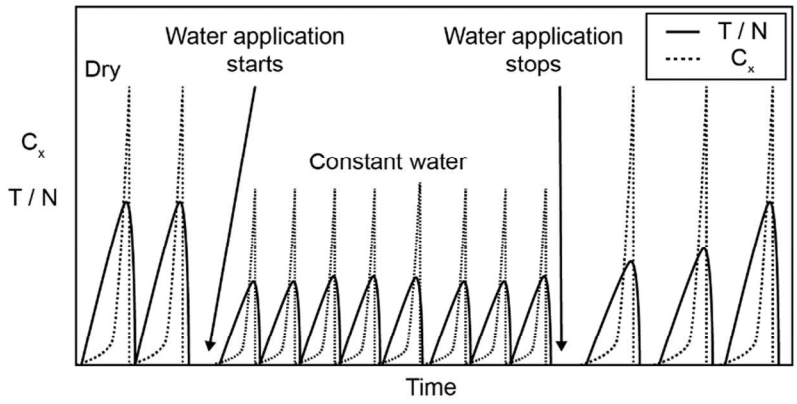

Figure 10: Constant water application using water droplet set-up test timeline schematic. Number of curves shown for illustrative purposes only

2.3 Test conditions

The investigation looked at the following wheel/rail third body conditions:

- Dry 'clean' contact
- Constant water + drying with compressed air (this stops water recirculating so is more representative)
- Bulk water application
- Constant low water application (droplets)

Table 2 shows the tests that have been carried out on the tram wheel rig. A normal load of 4kN produced an equivalent mean contact pressure of 700MPa. Tests sequences as shown for test numbers 1-12 are subdivided by load, as the load can only be significantly changed when the test rig is not running. Tests sequences for 13-15 were run as a single continuous test. Number of cycles shown and the number of cycles conducted can vary depending on the test. For example, additional cycles may be included if a steady state had not been reached under constant conditions.

Table 2: Table of tests on the full-scale tram wheel rig.

No.	Speed	Load sequence	Contact conditions
	[m/s]	Normal force [kN] (Cycles)	
1	5	4(5)	Dry (baseline)
2	5	4(5)	Water + drying with compressed air
3	5	4(A)	Bulk water application (60mL)
4	5	4(2dry)_4(15)_4(A)	Water droplet (25µL/s)
5	5	4(2dry)_4(15)_4(A)	Water droplet (35µL/s)
6	5	4(10)	Water pump (350µL/s)
A = run cycles until dry values of adhesion are measured.			

To map these water volumes to real world situations the equivalent amounts of rainfall has been calculated and plotted in Figure 11. The rainfall (mm/hr) is based on the assumption that the water is evenly distributed between the roller and wheel contact bands. The water volume is assumed to have been deposited over the

measured deposit width of 11 mm to give a combined area of 0.0558 m^2. This should only be treated as an estimation of the equivalent rainfall.

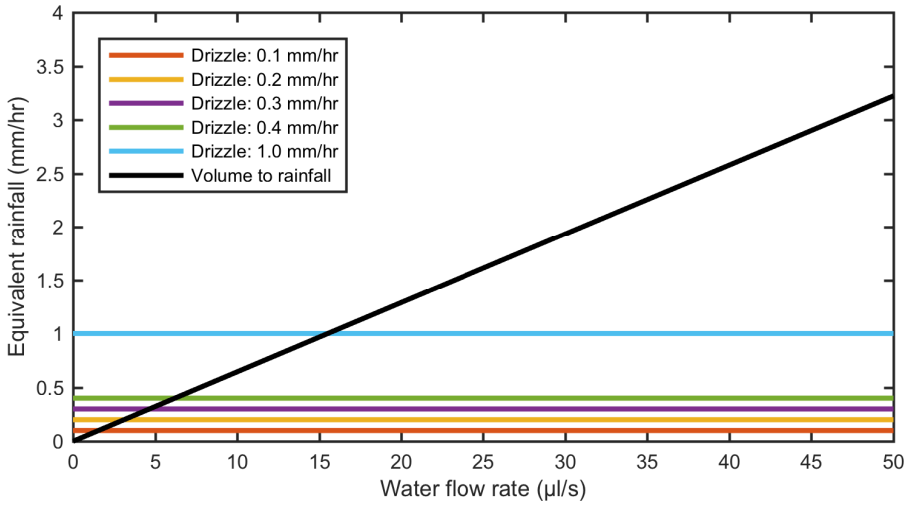

Figure 11: Estimation of the equivalent rainfall per hour against deposited water volume in full-scale tests. Solid black line shows the conversion of droplet application water flow rate into an equivalent rainfall in mm/hr. Horizontal lines do not relate to abscissa

3 Results

Tests were performed under all conditions in dry, bulk water application, constant water + drying with compressed air (Figure 6) and constant low levels of water application without drying with compressed air (Figure 7). All results shown in Figures 12 to Figure 15 have been plotted against dimensionless longitudinal creep c_x. Note that the creep range for Figures 12 to 14 is up to 50% (0.5) whilst Figure 15 and 16 are plotted to 100% (1.0).

Figure 12 shows the results under dry conditions. In dry conditions the peak adhesion is at a friction coefficient of 0.4. This level of adhesion is as expected for a dry rolling contact.

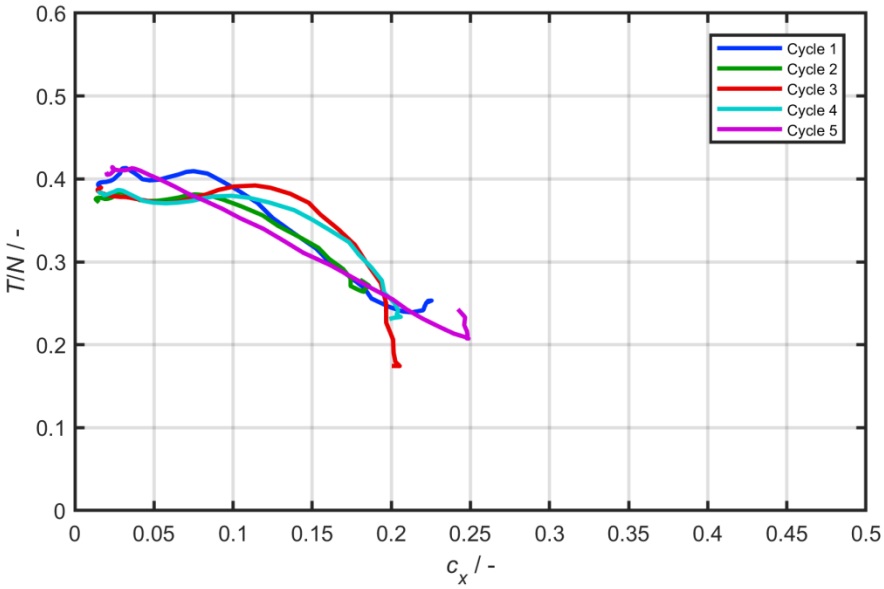

Figure 12: Creep curves from dry tests performed under 4 kN normal load and 5 m/s rolling velocity

Figure 13 shows the results from constant water plus drying with compressed air experiments. Water reduces the adhesion from dry levels to $T/N = 0.2$ as would be expected.

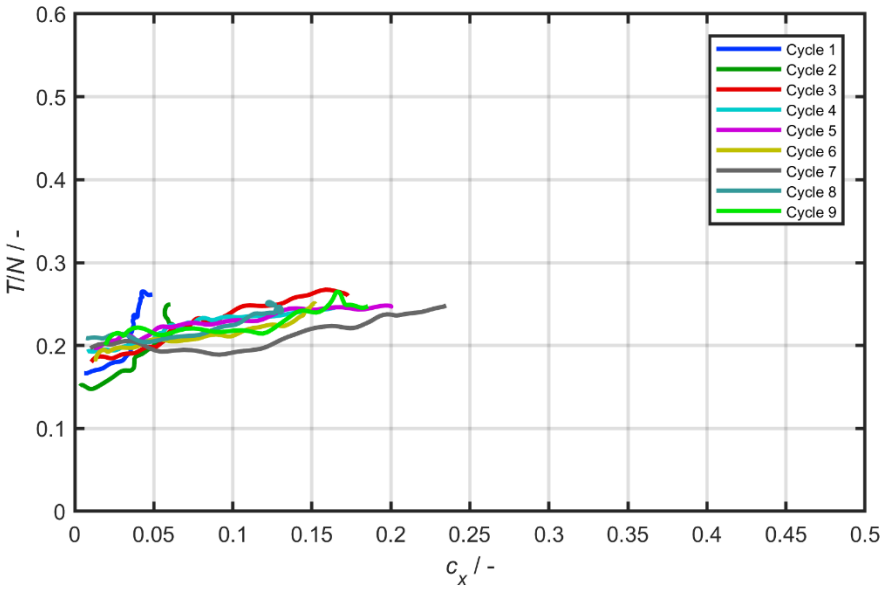

Figure 13: Creep curves from constant water (350 µL/s) + drying with compressed air tests performed under 4 kN normal load and 5 m/s rolling velocity

Figure 14 shows the bulk water application creep curves generated under a 4 kN load. The initial curves (dark blue and dark green) were generated under dry conditions. After water application was stopped there is a sustained level of reduced adhesion that can be seen in cycles 3 to 7, when water is still present on the roller. Once there is no longer any water in the contact dry levels of adhesion are again seen (cycles 8 and 9).

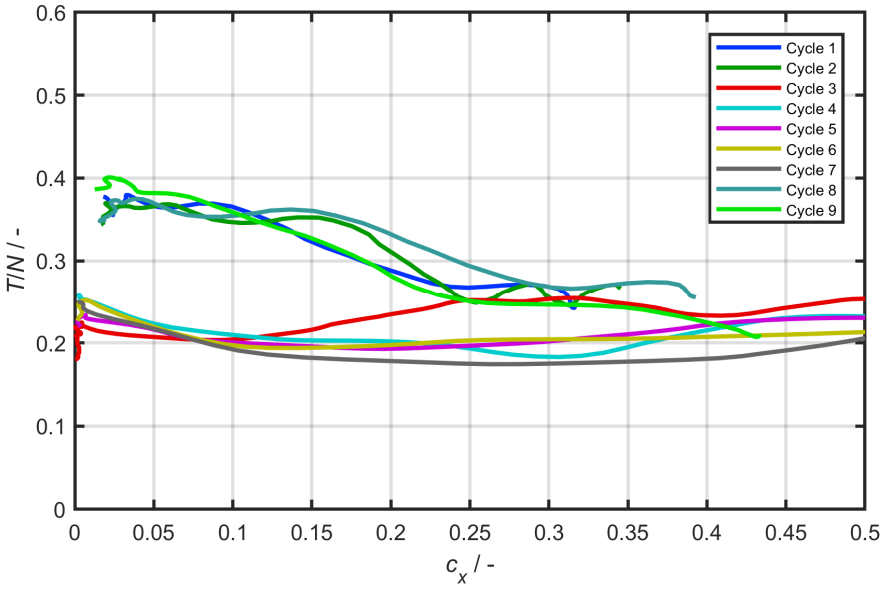

Figure 14: Creep curves from bulk water application (60 ml) tests performed under 4 kN normal load and 5 m/s rolling velocity

Figure 15 shows a sample of the curves generated using the water droplet application system at a rolling speed of 5 m/s. As water droplet rate is increased from 25 µl/s to 35 µl/s there is a clear change in adhesion behaviour. At the low water deposit rate there was a rapid decrease in adhesion upon sliding. The traction control system on the rig was unable to effectively return to pure rolling once sliding was initiated and high creepage rates were seen. Levels of adhesion were reduced to below 0.1 (T/N). The high water rate (350 µl/s) produced similar curves to those from bulk water application tests (see full wet curves from Figure 13).

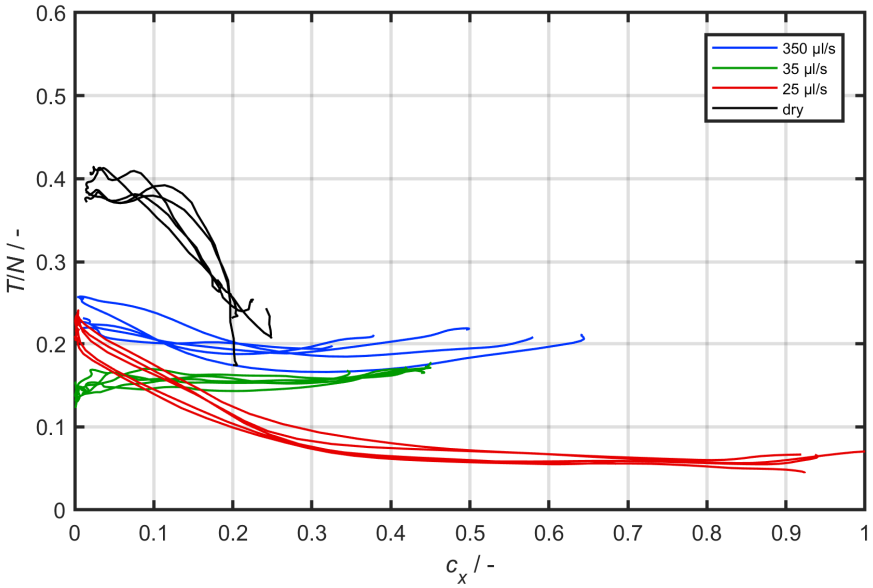

Figure 15: Creep curves from water droplet tests showing variation of water rate at fixed load and speed. Plot shows adhesion improvements as water rate is increased from a low value

During testing it was observed that an ultra-low level of adhesion (T/N ≈ 0.05) was measured as the wheel returned to free rolling when low levels of water (25 µl/s)

were applied to the contact. A comparison between a dry return curve and a return curve measured under the conditions shown to reduce adhesion above, can be seen in Figure 16.

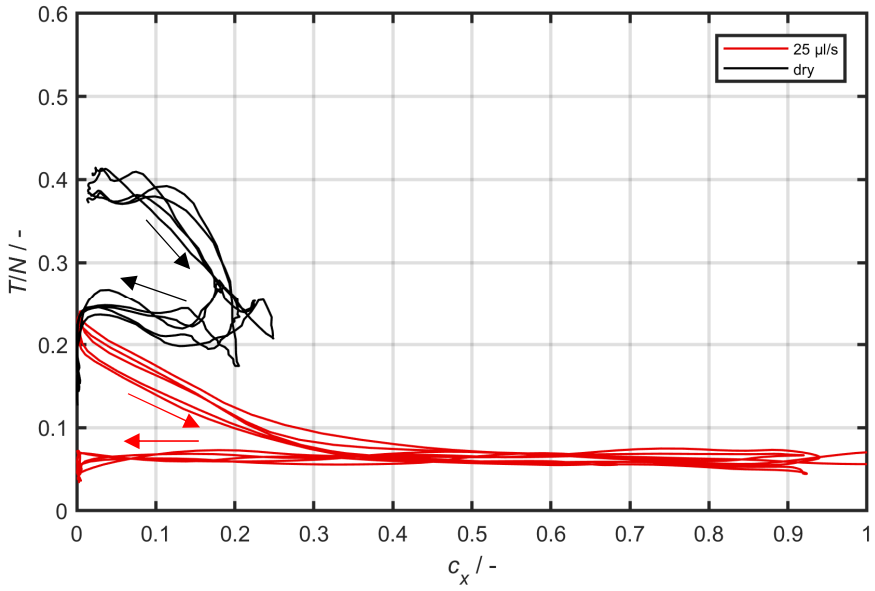

Figure 16: Creep curves and return creep curve in dry and wet condition. Adhesion is ultra-low during the return to rolling. Arrows indicate the direction of changing creepage

4 Discussion

From observing the contact patch during testing with small amounts of water the third body in the contact is clearly seen to change over the course of a test. Under water droplet tests with water sufficient to keep the surface wetted, a layer is clearly seen on the running band of both the wheel and roller. This layer is formed of oxides and wear debris generated from the contact and the added water (within a few cycles of the test starting).

As the amount of water is increased from zero to fully wet conditions the solid fraction (from oxides and wear debris) will decrease from 100 % (dry) to below the levels shown to reduce adhesion. This transition will have an effect on how the mixture is entrained into the contact with lower solid fractions (higher water) being cleared more readily whilst the higher solid fractions are sustaining the low adhesion. The friction values seen with fully wet conditions or for bulk water application relate well to data seen in previous tests with water in a rolling/sliding contact [3, 8].

To investigate the drying process under water droplet application, a video recording was made of a test where the water application was stopped and a set of curves ran until the contact patch was again dry. After stopping the supply of water to the contact, the third body layer begins to undergo a transition as it begins to dry out. This drying out process can be seen in the Figure 17 from (a) to (c), where the final image shows a clear running band, with wet debris still evident at the sides of the band.

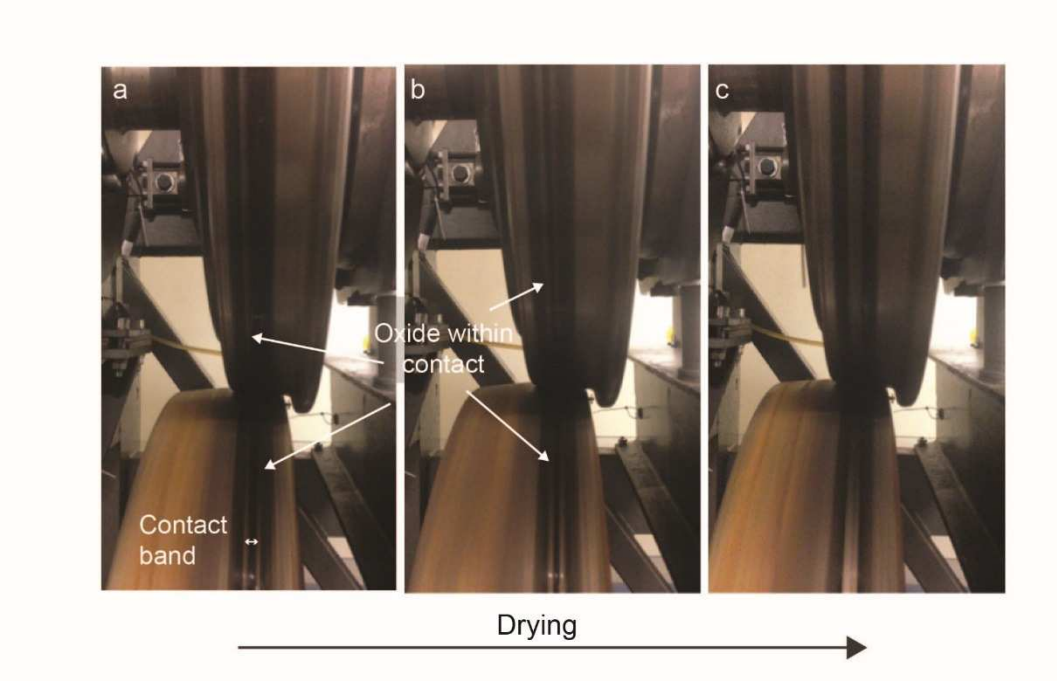

Figure 17: Appearance of contact patch during water droplet tests

The final removal of oxide from the contact happened over a very short period, perhaps only a few rotations of the rollers. It is likely that this is when the water/oxide mixtures are suitable for causing low adhesion. This period is too short to generate a full creep curve, unless the water supply is kept at the correct level to sustain the water/oxide mix. It is for this reason that the bulk water tests did not produce low adhesion even as the water amounts were steadily decreased.

The depth of the water film on the surface has been estimated from the volume of water deposited over the combined surface area of the roller and wheel surfaces. For simplicity it has been assumed that the water is not accumulated on the surface and the surfaces are perfectly smooth. The expected average surface roughness of the roller and wheel is 1 µm. As can be seen in Figure 18 the depth of water never exceeds the surface roughness in the range shown (up to 50 µL), which indicates that the amount water in the contact would not have separated the surfaces.

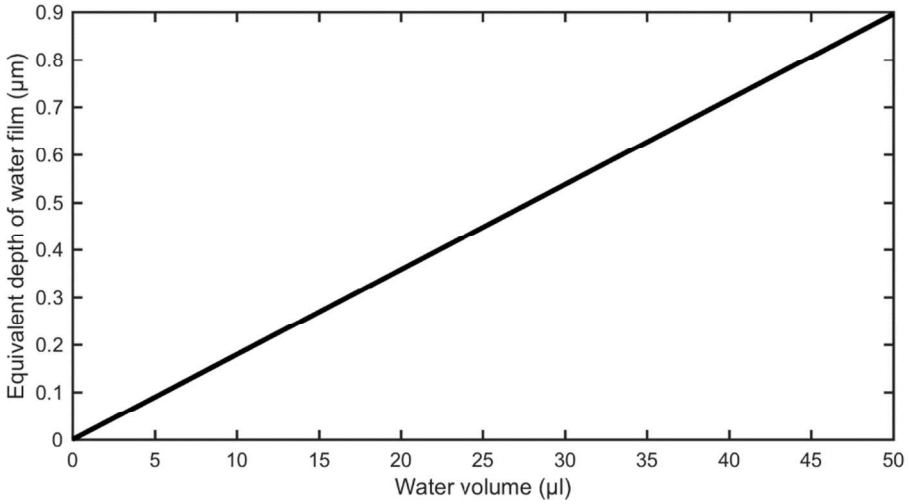

Figure 18: Estimation of the equivalent water depth formed on a flat surface for specific water volume. Estimated surface roughness in tram wheel rig 1µm

In the field, the wheel would be a fresh supply of contaminant sufficient to sustain low adhesion. When the water rate is increased from this low amount there is a transition phase up to fully wet curves.

The sustained low adhesion as the torque is backed off (shown in Figure 16) is very interesting as it ties up with anecdotal evidence from the field where slides are sustained even when power is reduced by a train driver. The T/N value increases as oxide is built up in the test and then reduces as the amount of oxide to water reaches the critical proportion (see Figure 3 for example). Once the slipping condition is occurring in the rig the torque is reduced. This means that there is less mechanical cleaning and therefore the effect can be extended. The outward curve could be equated to a wheel running on a rail where there is no corrosion/oxidation present, but perhaps precipitation is about to happen or the rail is drying out so small amounts of moisture are present. The oxide being generated in the contact due to the partial slip under load then reaches a critical level and adhesion reduces. The return curve could be what happens when a wheel runs on a rail head that is already oxidized due to moisture, perhaps, for example, when the first train of the day runs in dew conditions.

5 Conclusions

Tests on the full-scale rig have shown that when the right set of wet conditions are sustained once sliding is initiated adhesion levels are rapidly reduced to ultra-low levels (min(T/N) = 0.05). The low adhesion conditions are formed and sustained during sliding. This level of adhesion is on the boundary of low and exceptionally low adhesion as defined by Vasic et al. [13]. Furthermore, at low amounts of water the adhesion characteristics can chance suddenly between “dry” and “wet” mode.

Visual inspection of the contact band during tests indicated that the third body layer formed changes during tests when water is allowed to evaporate. The mixture is comprised of water, oxides and wear debris generated from the contacting bodies. It was observed that this oxide/water is fully removed during a few rotations of the rollers as the water evaporates. The short time span indicates there is a high chance

of missing this transition point during a test unless water application is constant (and at the right level to produce a viscous oxide water mixture). This is perhaps why others have not been able to generate such low adhesion conditions during testing.

Creep curves have been generated that can now be used in modelling to link water amount to friction levels in the wheel/rail interface (see for example Trummer et al., 2017) and for informing multi-body dynamics simulations of train behaviour in low adhesion conditions.

6 Acknowledgements

This work has been funded by the Rail Safety and Standards Board (RSSB) and Network Rail within project RSSB project T1077.

7 References

[1] White, B.T., Nilsson, R., Olofsson, U., Arnall, A.D., Evans, M.D., Armitage, T., Fisk, J., Fletcher, D.I., Lewis, R., 2018, “A Study into the Effect of the Presence of Moisture at the Wheel/Rail Interface during Dew and Damp Conditions”, *Journal of Rail and Rapid Transit, Proceedings of the IMechE, Part F*, Vol. 232, pp979–989.

[2] Ishizaka, K., Lewis, S.R., Lewis, R., 2017, “The Low Adhesion Problem due to Leaf Contamination in the Wheel/Rail Contact: Bonding and Low Adhesion Mechanisms”, *Wear*, Vol. 378-379, pp183-197.

[3] Chen, H., Ban, T., Ishida, M., Nakahara, T., 2008, “Experimental investigation of influential factors on adhesion between wheel and rail under wet conditions”, *Wear*, Vol. 265, pp1504-1511.

[4] Zhu, Y., 2018, “The Influence of Iron Oxides on Wheel-Rail Contact: A Literature Review”, *Proceedings of the IMechE, Part F, Journal of Rail and Rapid Transit*., Vol. 323, pp734-743.

[5] Zhu, Y., Lyu, Y., Olofsson, O., 2015, “Mapping the Friction between Railway Wheels and Rails Focusing on Environmental Conditions”, *Wear*, Vol. 324–325, pp122-128.

[6] Zhu, Y., Chen, X., Wang, W., Yang, H., 2015, “A Study on Iron Oxides and Surface Roughness in Dry and Wet Wheel–Rail Contacts”, *Wear*, Vol. 328-329, pp241-248.

[7] Zhu, Y., Olofsson, U., Chen, H., 2013, “Friction Between Wheel and Rail: A Pin-On-Disc Study of Environmental Conditions and Iron Oxides”, *Tribology Letters*, Vol., 52, pp327-339.

[8] Zhu, Y., Olofsson, U., Persson, K., 2012, “Investigation of Factors Influencing Wheel–Rail Adhesion using a Mini-Traction Machine”, *Wear*, Vol. 292–293, pp218–231.

[9] Buckley-Johnstone, L.E., Trummer, G., Voltr, P., Meierhofer, A., Six, K., Fletcher, D.I., Lewis, R., 2019, “Assessing the impact of small amounts of

water and iron oxides on adhesion in the wheel/rail interface using high pressure torsion testing", in press, *Tribology International*.

[10] Beagley, T.M., Pritchard, C., 1975, "Wheel/rail adhesion - the overriding influence of water", *Wear*, Vol. 35, No. 2, pp299–313.

[11] Trummer, G., Buckley-Johnstone, L., Voltr, P., Meierhofer, A., Lewis, R., Six, K., 2017, "Wheel-rail creep force model for predicting water induced low adhesion phenomena", *Tribology International*, Vol. 109, pp409-415.

[12] Voltr, P. and Lata, M., 2014, "Transient wheel–rail adhesion characteristics under the cleaning effect of sliding", *Vehicle System Dynamics*, Vol. 53, pp605-618.

[6] Vasic, G., Franklin, F., Kapoor, A., Lucanin, V., 2008, "Laboratory simulation of low-adhesion leaf film on rail steel", *International Journal of Surface Science and Engineering*, Vol. 2, pp84-97.